Precision and Accuracy of EO-1 Advanced Land Imager (ALI) Data for Semiarid Vegetation Studies

Andrew James Elmore and John Fraser Mustard

***Abstract*—Landsat Thematic Mapper (TM) data and spectral mixture analysis have been used to estimate vegetation green cover in the Great Basin, western United States, to ±4.0% green cover (%GC). In this paper, we compare estimates of percent green cover derived from EO-1 Advanced Land Imager (ALI) data to estimates derived from field-based analyses and to results derived from Landsat Enhanced Thematic Mapper plus (ETM+) data. These analyses define the precision and accuracy of ALI and ETM+ for making quantitative measurements of earth for semiarid ecological studies. The benefits of using ALI were not observed in the calculated uncertainty values (±5.61%GC and ±6.15%GC for ETM+ and ALI, respectively). However, ALI did not return as many negative green cover estimates and exhibited lower spatial variance in regions of low green cover. These results were attributed to the better signal to noise and data precision inherent to the ALI sensor, and not to the increased number of multispectral bands. ALI was found to be internally inconsistent in that the third sensor chip assembly image swath contained multispectral band coregistration errors. This caused a less than 25%GC error in the ALI estimate of percent green cover along large vegetation gradients.**

***Index Terms*—Environmental factors, remote sensing, spectral mixture analysis, vegetation measurement.**

I. Introduction

THE VAST extent of land-use and land-cover changes occurring around the world demands that the remote sensing community provide technologies capable of fast and effective land monitoring. Nowhere is this more applicable than in arid and semiarid lands where changes in water resources alter the landscape on a regional scale. Remote sensing techniques have become important for vegetation monitoring in these environments because fieldwork is difficult or impossible at scales useful for management [1]. In addition to vegetation change measurements, remote sensing observations can be useful in revealing gradients in vegetation cover that can be further shown to relate to precipitation, groundwater, or edaphic factors across the landscape [2]. However, for remote sensing to be a useful addition to traditional field techniques, any algorithm retrieving ecological information must be quantitative in nature and result in meaningful measurements of ecosystem qualities over time. When these criteria are met, remote sensing can be used to quantify gradients and spatial heterogeneity over large regions and through time, analyses that are difficult with field techniques alone [3], [4].

We have shown that vegetation cover estimates accurate to within 4.0% green cover (%GC) can be derived from Landsat TM data using spectral mixture analysis (SMA) [5]. This result was obtained by comparing concurrent Landsat TM and field data representing a variety of shrubland and meadow plant communities of the Great Basin, western United States and corroborates with laboratory-based analyses of soil–vegetation mixtures [6]. Furthermore it was shown that the SMA estimates were stable through time, with an estimated accuracy of 3.8% in determining %GC using six years of concurrent field and Landsat observations. SMA was found to be superior to vegetation indices such as the normalized difference vegetation index (NDVI) because it is minimally affected by variations in soil color and it results in a quantitative, physically meaningful, estimate of plant community condition. The need for consistent measurements of this type, which allow for an understanding of vegetation change through time, dictates that any Landsat follow-on instrument meet or exceed these performance values.

In this paper, we compare the capabilities of EO-1 Advanced Land Imager (ALI) data with the capabilities of Landsat Enhanced Thematic Mapper plus (ETM+) for measurements of vegetation cover. ALI is a nine-band 12-bit sensor and is, therefore, a higher technology sensor than Landsat ETM+, with presumed better focusing (smaller IFOV) and material discrimination abilities [7]. The nine bands of ALI were designed to cover the ETM+ bandpasses, while extending the total functionality. ALI includes two additional bands at 0.433–0.453 and 1.2–1.3 μm, and the ETM+ band 4 (near-infrared) is split into two bands. ALI is a pushbroom-type sensor, consisting of four sensor chip assemblies (SCAs). During a data collection event, each of the four SCAs collects an individual image and the user joins these images. Differences in sensor construction may also play a role in the capability of each sensor for ecological studies.

There are two approaches to sensor comparison. The first seeks to understand the fundamental differences between sensors through a band-by-band comparison of technological variables such as SNR, which relate to the sensor capabilities for material discrimination. The second approach utilizes an end-to-end analysis of land cover, and then compares the end products derived from each of two sensors. We take the second

Manuscript received July 3, 2002; revised March 5, 2003. This work was supported by the National Aeronautics and Space Administration Earth Observing 1 Science Validation Team under Grant NCC5-487.

A. J. Elmore was with the Department of Geological Sciences, Brown University, Providence, RI 02912 USA. He is now with the Carnegie Institution of Washington, Stanford, CA 94305 USA (e-mail: Andrew@elmore.cc).

J. F. Mustard is with the Department of Geological Sciences, Brown University, Providence, RI 02912 USA (e-mail: John_Mustard@Brown.edu).

Digital Object Identifier 10.1109/TGRS.2003.813132

approach, with the end goal of understanding the advantages and disadvantages of using ALI over ETM+ for ecological studies. For this comparison to be useful, a consistent methodology must be employed when processing and analyzing these data.

We analyzed concurrently acquired ALI, ETM+, and field data in pursuit of three objectives: 1) to determine the capabilities of ALI relative to ETM+ to calculate %GC of vegetation comparable with field based measurements using the spectral bands functionally equivalent to ETM+, 2) to determine the capabilities of ALI to calculate the %GC of green vegetation using the full complement of spectral bands and to compare these results to the capabilities of ETM+, and 3) more generally, to assess the capabilities of ALI and ETM+ to produce internally consistent multispectral images for quantitative analysis in ecological and land-use land-cover change applications. Our primary emphasis within these objectives was the comparison of remote measures of green cover with field-based analyses. However, throughout the analysis we draw out differences between the two sensor results, and in 3) we make a direct image-to-image comparison of scene spatial variability.

II. Method

The EO-1 ALI and Landsat ETM+ sensors each acquired one dataset on June 21, 2001 of Owens Valley, CA (Fig. 1). Due to the orbital positions of the EO-1 and Landsat satellites, these data were acquired only 1 min apart. This assured the data were functionally identical in terms of sun zenith and azimuth. Owens Valley, a semiarid basin located in eastern California, was chosen for this study because of our ongoing research activities in the region [5], [8]. Concurrent with these remote acquisitions, field data were collected by the Inyo County Water Department (ICWD) and the Los Angeles Department of Water and Power (LADWP) on percent green cover at 27 field sites. When possible, our methodology for the processing and comparison of these data followed our previous work [5]. From our previous work, we also bring forward a georeferenced Landsat TM dataset from September 1992.

Preprocessing

We reduced the nine-band ALI data to six bands, where each of the six bands was functionally similar to one of the six ETM+ bands. This was accomplished through the removal of the 0.433–0.453- and 1.2–1.3-μm bands, and the combination of the two NIR bands by averaging the values. Using high spectral resolution data of a Nevada saltbush (*Atriplex lentiformis* ssp. *torreyi*) shrub, we tested the validity of approximating the spectral response of ETM+ band 4 with the average of ALI bands 4 and 4p. The true spectral response of the two ALI bands was calculated and averaged, and then compared with the ETM+ response. The difference between these values was 0.179%, which would be within the noise of a sensor with a 500-to-1 SNR. From this analysis, we were confident that the average of bands 4 and 4p was a reasonable approximation of ETM+ band 4. Therefore, three datasets were used to meet our objectives: 1) ETM+ (six eight-bit bands), 2) ALI6 (six 12-bit bands, functionally similar to the ETM+ bands), and 3) ALI9 (nine 12-bit bands).

The ETM+, ALI6, and ALI9 data were coregistered to the previously georeferenced TM scene from 1992. In the case of the ETM+ data, we used a second-order polynomial, and automated ground-control-point-picking code to fit the data [5]. For the ALI data, we used a thin plate spline (TPS) algorithm [9]. The TPS algorithm fits ground control points exactly and then warps data around the points accordingly to achieve the best fit. We manually selected over 100 ground control points. The TPS algorithm was found to be an improvement over the second-order polynomial for coregistering ALI. Through the examination of road intersections and similar distinctive land features it was determined that the resulting interimage coregistration was within one pixel across the valley floor (where the field sites were located).

Spectral Mixture Analysis

A linear spectral mixture analysis (SMA) approach [3], [10] was taken using image-derived endmembers. Endmembers are unique spectra that are thought to represent basic components of the earth's surface, such as vegetation and soil types. In SMA, it is assumed that the spectrum retrieved from each pixel is a linear combination of endmember spectra. The summation of these endmember spectra, each multiplied by the proper fractional coefficient, results in a model pixel spectrum where the difference between the model and observation is the estimate of error. To the extent that sensor radiance is a linear combination of endmember radiance, the coefficient is an estimate of the fractional area of the pixel covered by that endmember [11]. In semiarid datasets, endmembers are typically vegetation, shade (to account for illumination and albedo effects), and one to three soils depending on the number of bands utilized by the sensor and the variability of soil reflectance among these bands.

The SMA algorithm is embodied in the following equations:

$$\mathrm{DN}_b = \sum_{i=1}^{N} F_i \mathrm{DN}_{i,b} + E_b \tag{1}$$

$$\sum_{i=1}^{N} F_i = 1 \tag{2}$$

$$\mathrm{rmse} = \sqrt{\sum_{i=1}^{B} \frac{(E_i)^2}{B}} \tag{3}$$

where DN_b is the intensity {e.g., radiance, reflectance, digital number (DN)} of a given pixel in bandpass or wavelength b; F_i is the fractional abundance of endmember i, $\mathrm{DN}_{i,b}$ is the intensity of image endmember i at wavelength b; N is the number of endmembers; and E_b is the error of the fit for bandpass b (referred to in this paper as the band b residual). For example, for the analysis with ALI data, there will be nine equations, one for each spectral band ($B = 9$). Equation (2) constrains the sum of the fractions to equal unity; however, there is no constraint that the fractions must be between 0.0 and 1.0. Allowing individual fractions outside the range 0.0–1.0 provides important information on the validity of endmember selection [12], [13]. Equation (3) is the total rmse where B is the number of spectral bands.

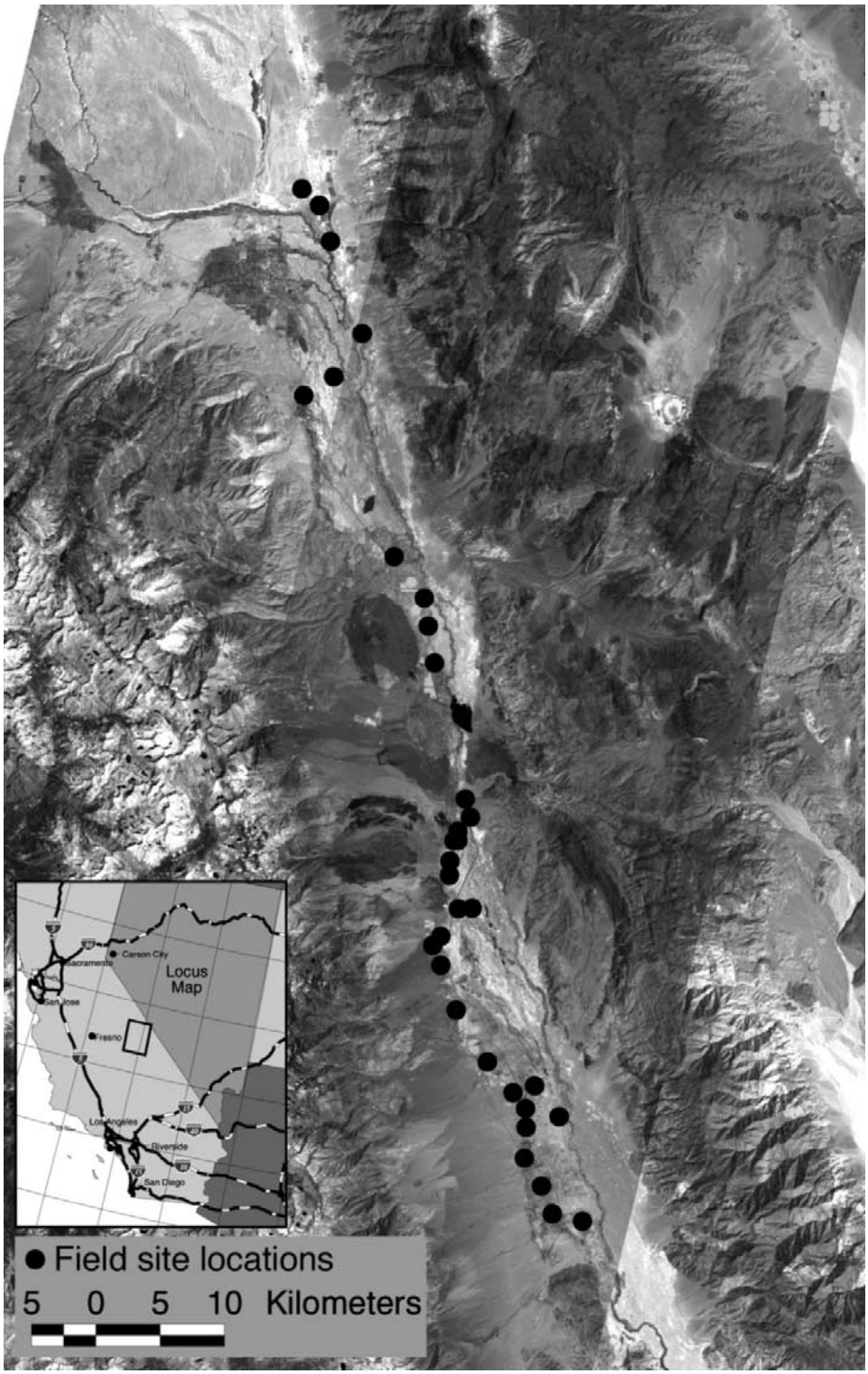

Fig. 1. EO-1 ALI data (center) and Landsat ETM+ (background) data from Owens Valley, CA, showing the locations of each of the datasets and the vegetation field sites used in this study. The field sites represented a variety of shrub and meadow plant communities.

An additional calculation can be employed to normalize the vegetation fraction to account for the fraction of shade calculated for each pixel [3]. This approach can be particularly useful in environments where the shade fraction is correlated with the vegetation fraction (i.e., the vegetation canopy is casting shadows on adjacent vegetation dependent on the sun angle). However, we have found that the shade fraction is often negatively correlated with soil brightness. When this is the case, there is no benefit to normalizing for shade because the resulting vegetation fraction becomes negatively correlated with soil brightness. Therefore, shade normalization was not employed in this study.

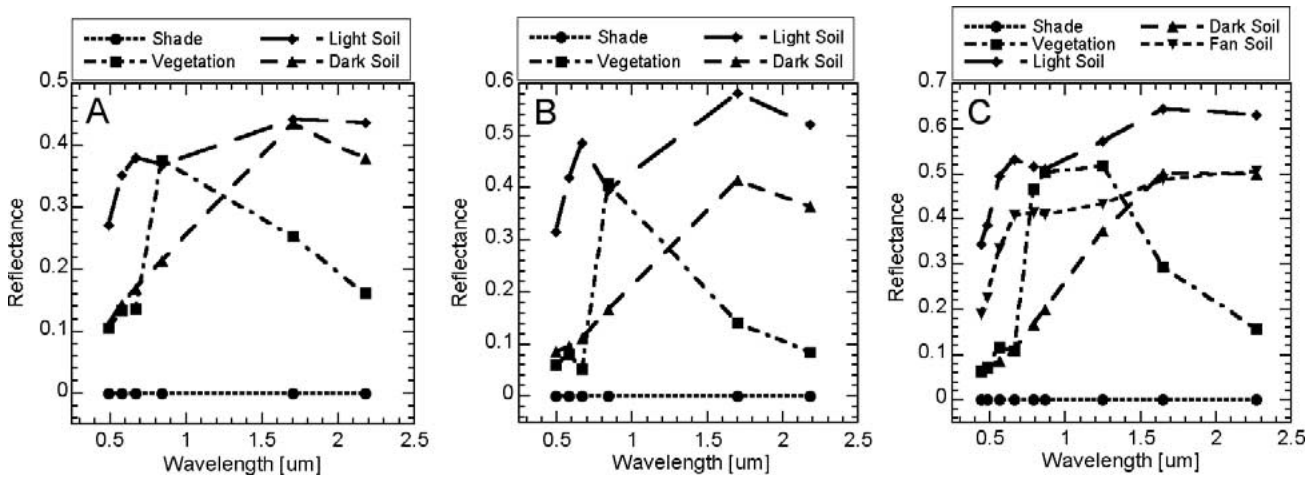

Fig. 2. There were three sets of endmember spectra used in this study. (A) Historic endmembers used in [5] were aligned with the current datasets (ETM+ and ALI6) to assess the capability of ALI to extend the legacy of ETM+. (B) ETM+ best case endmembers were image derived from the same types of features as the historical endmembers, but modeled total scene variance more efficiently. (C) ALI9 best case endmembers utilized all 9 bands and were, therefore, a better representation of the capabilities of ALI for estimating percent green cover.

Endmembers

The most critical step in SMA is the selection of endmembers. Endmembers must be representative of physical materials in the scene. They must also, through the mixture model, bound nearly all of the spectral variance of the scene, thus reducing the total rmse to a value close to the known noise level of the instrument. Additionally, band residual images [E_b in (1)] and rmse images must exhibit very little surface texture other than that due to sensor noise. For this analysis, we selected three sets of endmembers.

The first set we called the historic endmembers [Fig. 2(A)] because they were extracted from a 1992 Landsat-5 scene. These endmembers were used to model Landsat data of Owens valley, consisting of annual observations covering the past 17 years [5], [8], and thus, we have demonstrated that these spectra provide a robust set for quantitative modeling of the surface through time. The application of historical endmembers is important because of the need to maintain or improve accuracy through a consistent methodology with transitions to new sensors. If ALI, through SMA, cannot properly model the surface using the historical endmembers, then it will not be useful as a monitoring tool in studies such as ours in Owens Valley. The historical endmembers were reported by [5], and included 1) vegetation from a very well watered meadow close to the Owens River, 2) an alkaline (light) soil from the valley floor, 3) a dark, organic-rich soil from a meadow community, and 4) shade [Fig. 2(A)].

The historical endmembers are image derived and have not been corrected for atmospheric effects. Therefore, we aligned the endmember spectra to the radiometric variance inherent to the newly acquired data before performing SMA. Four temporally invariant surface features (TISFs) were identified on the valley floor. These included both light and dark surfaces and were not vegetated. Band-by-band, the radiometric response from these surfaces in the 1992 ETM+ data acquisition was regressed against the surface response identified from the current datasets. In this way, a set of gain and offset correction factors were calculated for the ALI6 and ETM+ data. These values were then used to align the historical endmember spectra to the image data before SMA was performed. Spectral alignment of endmember spectra relieves the need for atmospheric removal and does not alter the spectral characteristic of the data. Spectral alignment is the only way vegetation fraction results derived using SMA can be compared between images, especially through time [14], [15].

Historic endmembers allow us to make a direct comparison of vegetation estimates between images. This analysis demonstrates the capabilities of ALI to continue the legacy of Landsat TM and ETM+ for measuring vegetation change through time. However, it is possible that the historic endmembers would not model the scene's spectral variance with the same efficiency as endmembers particular to the new observation. This is an uncertainty we must accept when we attempt to measure vegetation change. But, there is an issue of bias if we chose endmembers from Landsat data and then draw conclusions from how well they perform when applied to ALI data. For a best case analysis, image endmembers should be chosen from the dataset they are applied to using SMA, which relieves the need for spectral alignment of the endmember spectra to scene radiometry. For these reasons, we selected a second set of endmembers representing the best case scenario for the Landsat ETM+ data. These four endmembers [Fig. 2(B)] were selected from the same types of surface cover used to define the historic endmembers. However, the new endmembers resulted in a lower rmse and lower band-residual errors.

For comparison with the best case ETM+ endmembers, a third set of endmember spectra were selected from the ALI9 data (ALI best case scenario). A fifth endmember representing alluvial fan soils on the western side of Owens Valley was required to achieve an acceptable solution. The requirement of this additional soil endmember was not unexpected, as SMA solutions using TM and ETM+ data suggested a component of unmodeled spectral variance in these soils, but was unresolved with the bands of TM or ETM+. This was the first apparent advantage of using ALI data over TM or ETM+, because it provided confidence that the total scene variance was being modeled by the endmember spectra.

Using SMA, we analyzed ETM+ data with historical and ETM+ best case endmembers (two separate analyses), ALI6 data with the historical and ETM+ best case endmembers (two separate analyses), and ALI9 with the ALI best case endmembers (one analysis). In the case of the ALI6 data analyses, we always aligned the endmember spectra (using the TISF-derived correction factors) to the data prior to running SMA. This process assured that the endmembers were appropriately scaled for use with ALI data, without altering the radiometry of the data.

Comparison With Field Data

Field data was collected at 33 field sites across Owens Valley between the days of June 17 and June 28 by ICWD and the LADWP. Twenty-seven of these sites fell within the ALI image. At each site, percent green cover was recorded using the point-frame method along 100-m transects. This method involves positioning a metal frame supporting vertical pins over the shrub and grass canopy [16], [17]. Pins are lowered through the frame at 33-cm intervals and the material the tip of the pin hits first is recorded. The percent of these pins (totaling 334) that hit green vegetation is recorded as the %GC. Multiple measurements of the same field site were used to estimate the uncertainty in making a single measurement at ± 2.3%GC [5].

Two grass species and three shrub species, all phreatophytes, dominated the field sites. The grass species were saltgrass (*Distichlis spicata*) and alkali sacaton (*Sporobolus airoides*), and the shrub species were Nevada saltbush (*Atriplex lentiformis* ssp. *torreyi*), rabbitbrush (*Chrysothamnus nauseosus*), and greasewood (*Sarcobatus vermiculatus*). Depth-to-water (saturated soil) at these sites ranged from -1 to -5 m and greatly influenced vegetation cover, which ranged from 3%GC to 52%GC and averaged 22.3%GC [18], [19].

After running SMA on the image data, each field site was located in the image and the %GC values for a square of 4 pixels were extracted from the vegetation fraction results. Great care was taken in locating each field site in the image data employing GPS and air-photographs [5]. In some cases, the field sites were located along gradients in vegetation cover where the correspondence between field and remote measurements of cover was sensitive to the determined site location.

Image-to-Image Comparison

As mentioned in the Introduction, one advantage of using remotely sensed data over field data is the capability to study spatial variability and gradients in vegetation cover that may relate to biophysical processes. ALI data, with a higher data precision (12-bit versus eight-bit) and higher signal-to-noise particularly for low radiance, is potentially of greater use in these types of studies. To test this idea, the spatial standard deviation (STD) of the vegetation estimates resulting from the two sensor data was compared in two ways. First, the STD of %GC values was calculated for the area surrounding each field site location (one pixel radius). And these values were evaluated as a function of the total %GC measured in the field at each site.

Second, we compared %GC and spatial STD of %GC across a gradient in vegetation cover for each of the two sensor results. An elevational gradient was located along the alluvial fans on the western side of the valley where vegetation increases with increasing elevation due to greater precipitation at higher elevations [2]. Vegetation cover ranged from less than five to about 35%GC along this gradient and no man-made structures (roads, fences) appeared to intersect the established profile. A one-pixel-wide profile was sampled from the ALI and ETM+ SMA results using the historical endmembers. We then calculated the STD for every five pixels along the profile and compared the sensor results.

Finally, we made a general assessment of the SMA results using each of the two sensors. Through SMA, band residual images were produced and evaluated for consistency and sensitivity to endmember selection. When endmembers are appropriately chosen, band residual images and total rmse images [see (3)] exhibit few signs of surface features. By comparing the band residual and rmse images between sensor results, we made an integrative assessment of SMA as an investigative tool using ALI and ETM+ data.

III. Results

Our results compare the capability of each sensor to estimate vegetation cover. In each case, this capability is assessed relative to the field results, but the field results have inherent limitations. Therefore, we have treated each of the techniques as an independent measurement. We then directly compare results derived from each sensor in an image-to-image comparison of the spatial STD and band residual values across the entire region.

Historic Endmembers

The use of historic endmembers allows us to determine the capability of the ALI sensor to continue the legacy of the Landsat sensors. For each sensor, we have plotted the SMA results against field results from the 27 field sites (Fig. 3). SMA and field estimates of vegetation cover are measurements of the same quantities. Therefore, if SMA were perfect at representing field-based measurements, all of the data would fall along the 1 : 1 line. We have drawn the 1 : 1 line through the data on each of the plots (thin line). However, the data do not always fall on the 1 : 1 line, and instead follow a line parallel to the 1 : 1 line, but offset from it. This offset, which represents a bias in the measurements (on the part of either SMA or the field technique), was also seen in our previous work where it had the same sense: the SMA %GC estimates were typically lower that the field measurements. To illustrate the bias for each relationship we have drawn a line parallel to the 1 : 1 line at a distance equal to the average bias value.

A comparison of these results reveals that ALI performed slightly better than ETM+ through several types of assessment: 1) the average distance from the 1 : 1 line is smaller for ALI (3.80%GC for the ALI data and 7.23%GC for the ETM+ data); 2) there are fewer negative vegetation estimates reported using ALI data (one negative value) than using ETM+ data (eight negative values); 3) the STD of the data points from the bias-corrected 1 : 1 line is similar for the two sets of results, but smaller for the case using ALI (7.01%GC for ALI and 7.43%GC for ETM+). In 3), we are quantifying the average deviation of the

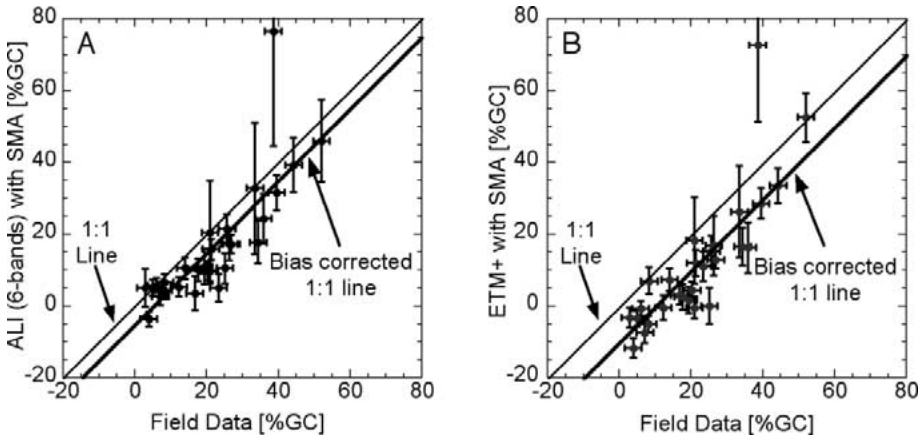

Fig. 3. Comparison of (A) ALI6 and (B) ETM+ for the estimation of percent green cover using SMA and historical endmembers reveals the capability of ALI to extend the legacy of the Landsat sensors. Note the near lack of negative vegetation cover values reported by ALI and the shorter error bars reported by ETM+ at high percent green cover values. In addition, ALI exhibited a smaller bias than ETM+, as indicated by the space between the two lines drawn on each plot (bias values are summarized in Table I). Error bars are derived from the mathematical error in the SMA model, the sensitivity of the model result to the spectral alignment of endmember spectra to the image data, and the uncertainty in our knowledge of field site location within the image data. See [5] for a more detailed description of error-bar calculation.

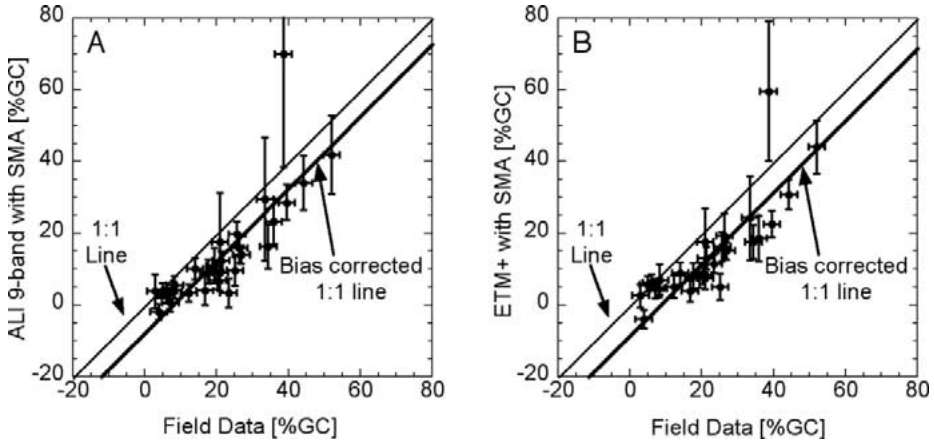

Fig. 4. Comparison of ALI9 (A) and ETM+ (B) for the SMA estimate of percent green cover using the best case endmembers for each dataset reveals the best result for each sensor using this technique. ETM+ and ALI return very similar results when best case endmembers are used, indicating that despite extra multispectral bands and 12-bit precision, ALI does not report vegetation cover values with better accuracy or precision for specific field sites.

TABLE I
DATASETS AND ENDMEMBERS USED IN SPECTRAL MIXTURE ANALYSIS. [1]OFFSET FROM THE 1 : 1 LINE. [2]STANDARD DEVIATION FROM THE BIAS-CORRECTED 1 : 1 LINE. [3]FROM [5]

Sensor	# of Bands	Data	Endmembers Applied	Bias[1]	STD[2]
Landsat ETM+	6	8-bit	Historic	7.23	7.43
Landsat ETM+	6	8-bit	ETM+ best-case	5.58	5.61
EO-1 ALI	6	12-bit	Historic	3.80	7.01
EO-1 ALI	6	12-bit	ETM+ best-case	4.97	6.15
EO-1 ALI	9	12-bit	ALI best-case	5.16	6.44
Landsat TM[3]	6	8-bit	Historic	1.88	3.96

data from the relationship between the SMA and field results. In past work, we have used this value as the uncertainty in using SMA to estimate field-based measurements of %GC. These results indicate that ALI produces values with similar uncertainty to ETM+ when historic endmembers are used, but exhibits advantages in terms of the number of negative values reported and the average bias from the 1 : 1 line.

Best Case Endmembers

The use of historical endmembers is illustrative for determining the worth of ALI for continuing the legacy of the Landsat sensors. However, for reasons outlined in the endmember section above, we selected new endmembers from each dataset and performed SMA. The best case endmembers resulted in a lower rmse and lower individual band residuals when applied to each sensor and, therefore, represent a comparison of sensor capabilities under an ideal analysis.

The SMA results using best case endmembers reveal that when appropriate endmembers are chosen independently for each of the two sensors, the results are similar (Fig. 4). As an indication of this statement, the average bias from the 1 : 1 line is similar for each dataset. Additionally, there is only one negative value each for ALI and ETM+; however, relative to the ALI result, ETM+ resulted in a lower STD from the bias-corrected 1 : 1 line (Table I). We also applied the ETM+ best case endmembers to the ALI6 dataset (not plotted), and noted that these results were very similar to the ETM+ best case results.

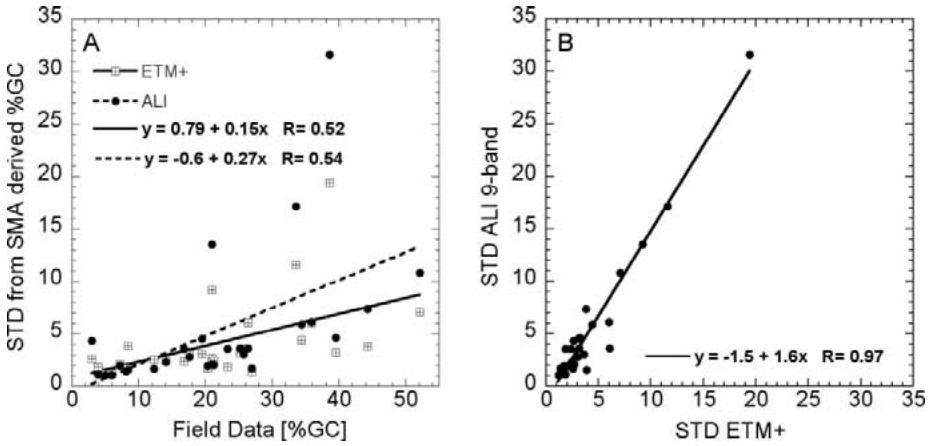

Fig. 5. (A) Spatial standard deviation (STD) of %GC surrounding each field site plotted against the %GC measured in the field exhibits an increasing relationship for both sensor results using best case endmembers. In (B), the STD value for each field site from each sensor result is compared. Together, (A) and (B) demonstrate that spatial variability in vegetation cover increases with total cover, and that the ALI result is more effective at detecting this trend.

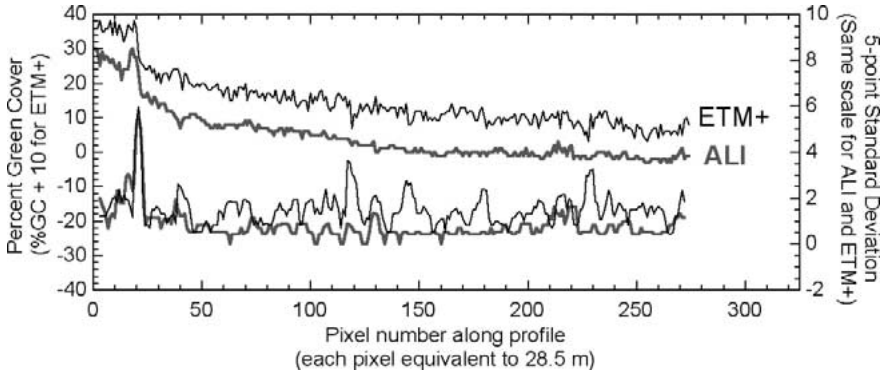

Fig. 6. When %GC as measured by the two sensors is compared along a profile from low cover to high cover the differences in spatial variability are profound. ALI consistently reports less noise between adjacent pixels than does ETM+ at low green cover. However, at high green cover ETM+ and ALI are more similar, as indicated by the five-point running standard deviation. For this figure, the SMA results using the historical endmembers are presented, but this result was independent of endmember selection.

Table I summarizes the results by providing the mean bias from the 1 : 1 line and the STD about the 1 : 1 line for each SMA result. Despite some variation between the results for each dataset, all bias values were $<$7.23%GC and STD from the 1 : 1 line were $<$7.43%GC. There were no large and consistent differences between ALI and ETM+ results using this measure. The STD for the best case endmembers for the ALI data was 6.44%GC. The offset value can always be subtracted and is also removed when measuring year-to-year change (by subtracting data from two consecutive years) [5]. Therefore, we can use this value as an uncertainty in finding a unique 1 : 1 relationship between SMA results and field results. If we believe field measurements represent the true %GC, then the STD from the 1 : 1 line is also the uncertainty in measuring percent green cover with SMA (i.e., $\pm$6.44%GC).

Image-to-Image Comparison: Analysis of Variance

Many factors likely influence spatial STD at the field site locations, but total %GC was found to be one important determinant [Fig. 5(B)]. From air photographs we also observed that the proximity of roads, irrigation ditches, and other man-made structures added additional spatial variability at selected sites. It was not a direct objective of this paper to identify the factors influencing spatial variability in %GC. Instead, we make the conjecture that spatial variability (measured as spatial STD) is an important observation for the remote sensing ecologist. Therefore, we compare the spatial STD reported by each of the sensors to assess the worth of each sensor for this type of measurement.

Fig. 5(A) demonstrates that the trend toward higher STD at sites with high %GC is more pronounced in the ALI results. The difference between the two sensor results is clearly exhibited when the STD values from each sensor result are directly compared [Fig. 5(B)]. ALI reports higher STD values than ETM+ and the difference between the two sensors scales with total variability. A comparison of Fig. 5(A) and (B) reveals that the spatial STD at a site is greater for ALI at all sites, nearly independent of total %GC. However, at several low cover ($<$15%GC) sites ETM+ reports larger spatial STD [Fig. 5(A)]. In Fig. 5(B), this effect is represented by the negative y axis intercept value, which is calculated from the linear regression between the two sensor results ($p < 0.001$).

We also investigated the variability in vegetation cover along a profile that extended across a vegetation gradient (Fig. 6). When vegetation cover was low ETM+ exhibited greater variability along the profile than did ALI. This difference is less pronounced at higher green cover values. The profile did not extend into a region of green cover $>$35%; however, the pattern

as seen at this range in %GC supports the result that ALI exhibits lower variance at low green cover and higher variance at high green cover than does ETM+. This pattern is again evident in the five-point running STD values along the profile (Fig. 6). The STD of the ETM+ results is greater than that for the ALI result at the low cover end of the profile. However, when cover reaches values above 10%GC, the STD values are more similar.

Image-to-Image Comparison: Internal Consistency

Comparison of the ETM+ and ALI data revealed inconsistencies in the multispectral (MS) band coregistration within the ALI data. The MS band 3 (the 0.63–0.69-μm band) residual [E_4 from (1)] exhibits the effects of this inconsistency (Fig. 7). Circles in the figure are center-pivot irrigation agricultural fields and, therefore, exhibit steep changes in vegetation green cover around their boundaries. These boundaries form white and black pairs in SCA-3 but not in SCA-4, indicating a problem in ALI band-to-band registration.

In an attempt to determine the influence of the band misregistration on the SMA results, we compared the vegetation estimates retrieved along the transect highlighted in Fig. 7. This transect crosses a center-pivot agricultural field and is located within the overlap region of SCA-3 and SCA-4; therefore, we directly compared results from the two SCAs. We also compare vegetation estimates with the difference in MS band 3 residual between the SCA-3 and SCA-4 along this transect (Fig. 8). The residual difference calculation is SCA-3 minus SCA-4 residual, which has the effect of removing the nominal (SCA-4) band residual and emphasizing the SCA-3 band residual.

Green cover estimates from the two SCAs are similar, but at the edges of the agricultural fields the two estimates separate up to 25%GC. For pixels with a high SCA-3 band residual SMA results in an underestimation of %GC. When SCA-3 reports a low value, the opposite is true, and the %GC is overestimated. This pattern is evident across the entire transect, and not only at the single points where the SCA-3 band residual is much greater than the SCA-4 band residual. At these single points, we are seeing the effect of error in the coregistration between the two SCAs. Considering that the pattern between the vegetation estimates and the band-residual difference is consistent across the entire length of the transect, we believe the result is robust and can be extrapolated to other regions of the image. The multispectral band misregistration would cause the largest discrepancy in the vegetation estimates reported by SCA-3 wherever low green-cover regions are located adjacent to high green-cover regions (i.e., steep vegetation gradients).

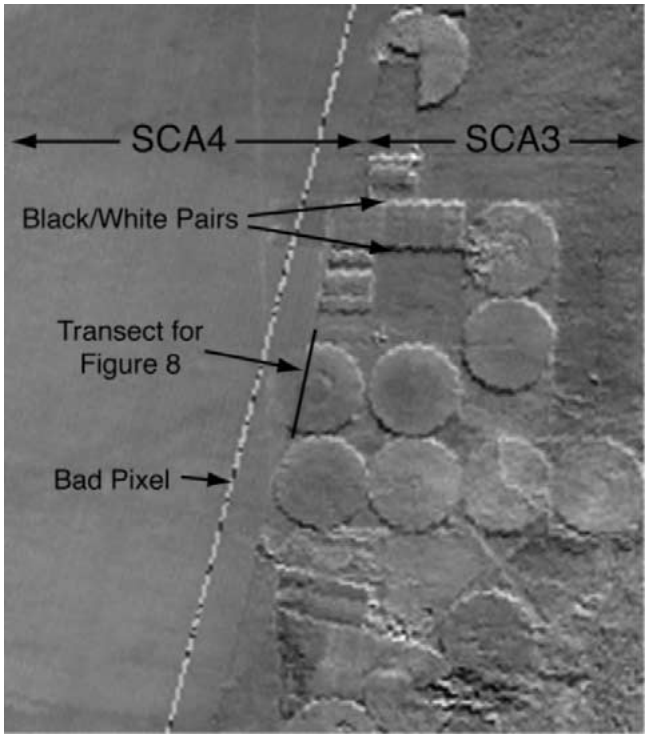

Fig. 7. Band 4 residual image [E_4 from (1)] showing the effect of a multispectral band misregistration in SCA3, but not SCA4. The center-point-irrigation fields clearly identifiable in the SCA3 part of the image do, in fact, extend into SCA4, but they are not visible in the image.

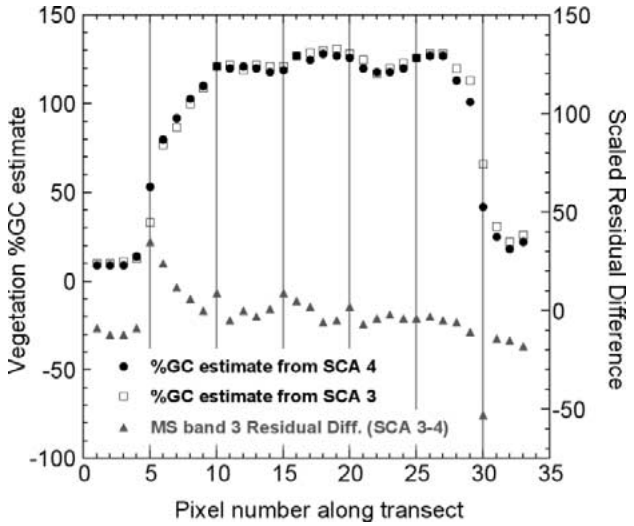

Fig. 8. Difference between the SCA3 and SCA4 MS-band-3 residual highlights the white/black pair apparent at the boundaries of the center point agricultural field from Fig. 7. In the pixels returning high SCA3 MS-band-3 residual, SCA3 underestimates the green cover by as much as 25%GC. Conversely, in pixels returning low SCA3 MS-band-3 residual, SCA overestimates the green cover. This pattern is apparent across the entire transect.

IV. Discussion

The accuracy of all results was less than reported in [5], but in the previous study six years of data and 33 monitoring sites (198 observations) were used. Because of the narrower image extent and the fact that ALI has only been in orbit for one year, we were only able to use 27 sites and one year of data for this study. Adding additional measurements of the same field sites (different collection dates) would conceivably reduce the average bias from the 1 : 1 line. Another difference is the time of year the study was conducted. In [5], the remote and field-based observations were made in August versus June for the current study. This difference may be important as total green cover, variability in green cover, and species proportions are changing throughout the summer months.

Despite the differences between the two analyses, the direction of the offset was the same for this study as for that reported by [5] and the uncertainty values calculated were within a factor

of two (Table I). Additionally, these results corroborate with the results from other field studies [3], [4] and laboratory studies [6]. It is becoming increasingly apparent that vegetation measurements derived from SMA, though demonstrating measurable uncertainty, are reliable estimates of the true land cover. Furthermore, our previous work has shown that the bias observed between SMA and field results is removed in a measurement of change in cover (the bias varies little through time for each field site). When vegetation change is the key variable of interest, SMA provides a robust tool for ecological studies.

The results of this paper demonstrate that in future work it would be valid to substitute ALI data, or data from a similar sensor, for ETM+ data without loss of quality in the end vegetation estimates. This is a significant result because it indicates that it is SMA (the method) and not the sensor data that limits our ability to accurately measure vegetation cover in these environments. Factors such as nonlinear reflectance effects [20], [21] and the effects of soil brightness and color [6], [22] have been repetitively cited as plausible causes of uncertainty in vegetation measurements. These factors may limit the capability of SMA for vegetation measurements, but variations on the technique have repetitively been used with great success [2], [3], [23]–[26]. Therefore, it is our opinion that the limitations of this method do not restrict its use for ecological studies, particularly in an analysis of change [8].

A comparison of the plots in Fig. 3 reveals that ALI returned only one negative green cover value and ETM+ returned eight negative values. This is a remarkable result and, if consistent across multiple datasets and through time, would indicate a significant benefit of using ALI data over ETM+ data. Negative values become less important in a measure of change, and can often be avoided through the selection of appropriate endmembers (e.g., our best case endmembers). However, when it is necessary to use the same endmembers in multiple images or when measures of absolute green cover are desired, negative values are nonphysical and are therefore difficult to interpret. For the data in Fig. 3, the same endmembers were used in the analysis of each sensor data and they each had the same number of bands. Therefore, there are only two differences between the datasets that could have resulted in fewer negative cover estimates. The first difference is the increased data precision associated with data dimension (12 versus 8 bit) and SNR, which may have given ALI the added precision to discriminate correctly between low cover sites.

The second difference is the position of the near infrared band. The fourth band of the six-band ALI dataset was created through averaging MS band 4 (0.775–0.805 μm) and 4p (0.845–0.890 μm). Although similar, this is not the same as the ETM+ band 4 (0.75–0.90 μm). Our analysis of the sensitivity of the combined ALI band 4 suggested that there would be very little difference between this band and ETM+ band 4. However, the ALI band 4 and 4p combination avoids the water absorption feature between 0.805–0.845 μm and, therefore, would be less sensitive to variations in atmospheric water across the scene. Increased water vapor at the field site relative to the sites used in the spectral alignment process would lower the measured radiance in the near infrared, thus forcing SMA to return negative vegetation values for those pixels. Future work will investigate the effect of water vapor on vegetation measurements using this method.

In the second component to this study, we performed a direct comparison of the spatial variability detected by the ALI and ETM+ sensors. The primary conclusion was that the spatial variability reported by the two sensors was not the same at all levels of homogeneity. First, at low spatial variability (homogeneous surfaces) ALI reported lower variability than did ETM+. This phenomenon was best observed in Fig. 6, where ALI-derived vegetation measurements across a low-cover bajada exhibited very low scatter. We believe this to be a result of better precision inherent to the ALI data, which would conceivably reduce the scatter in the vegetation measurement. Second, at high spatial variability (heterogeneous surfaces), ALI reported higher variability than did ETM+. This was best seen in the relationship between the two sensor results when comparing the STD of vegetation cover extracted from pixels surrounding the field sites [Fig. 5(B)]. In the semiarid landscape, it is common to find that surface heterogeneity is positively correlated with total cover. We found this to be true at our field site locations: the spatial variability detected by ALI at high cover sites was greater than that detected by ETM+. The capability to correctly separate adjacent pixels of varying vegetation cover is determined by the IFOV of the sensor, which is smaller for ALI than for ETM+. This feature apparently helps to identify spatial variability when it exists at the pixel scale. When phenomena related to spatial variability are of ecological interest, ALI is clearly a better sensor to use in their study. Finally, the difference in spatial variability detected by each of the two sensors was independent of endmember selection or the number of bands used in the analysis. Therefore, the precision of the sensor data and the IFOV (as described above) are the only remaining sensor parameters that can be proposed as a plausible explanation for this effect.

The issue of variations in the consistency of the ALI data between SCAs is potentially important for ecological studies using this method. The white and black pairs seen in Fig. 7 are clearly due to a misregistration of the multispectral bands in SCA-3. We have investigated the original data and noted the miss registration. However, we are aware that a leaky-pixel correction algorithm has been applied to this band of SCA-3 [7], [27] and that this algorithm may be related to the misregistration. We identified up to 25%GC differences between the SCA-3 and SCA-4 estimates of green cover along a steep vegetation gradient (Figs. 7 and 8). These results indicate that the inconsistency will cause mismeasurements of vegetation cover in regions of high spatial variation of vegetation cover, and effects will be minimal on vegetation estimates in homogeneous regions. Therefore, we recommend that the influence of the inconsistency in SCA-3 be assessed on a case-by-case basis and that researchers using these data be aware that it might have consequences for their work.

V. Conclusion

The ability to make consistent measurements of percent green cover in the arid regions of earth through time is critical for monitoring and understanding vegetation change. Spectral mixture

analysis continues to provide this capability, by producing accurate measures of percent green cover. When applied to ALI data, SMA returned estimates of vegetation cover that were comparable to field measurements and to values returned by ETM+ data. ALI reported lower variance in %GC estimates across targets with low spatial variability and fewer negative values in regions of very low cover. These benefits appear to be the result of better signal-to-noise and higher data precision inherent to ALI, because the results were invariant under the number of bands used in the analysis. ALI also exhibited greater sensitivity to variations between pixels, particularly in regions of high vegetation cover.

Overall, it is a result of this paper that the technological improvements built into ALI were realized in the precision and accuracy of the derived vegetation measurements. However, the improvements exhibited by ALI were only incremental, which suggests that inherent limitations of the method (SMA) applied to multispectral data of this type limit the ultimate accuracy of derived vegetation measurements. Nonetheless, SMA provides a reliable measurement of %GC that, using the methods of [5] is consistent over time, and highly beneficial for analysis of change [8]. Our results indicate that there are advantages in using ALI over ETM+ in terms of lower sensor noise and the ability to more completely model the spectral variance of this semiarid region with the additional spectral bands.

ACKNOWLEDGMENT

The authors thank staff at the Inyo County Water Department (S. J. Manning in particular) and the Los Angeles Department of Water and Power for providing the field data on vegetation cover necessary for this work. Finally, this work required the expertise and hard work of the EO-1 instrument and operation teams and the excellent leadership of S. Ungar.

REFERENCES

[1] P. T. Tueller, "Remote sensing science applications in arid environments," *Remote Sens. Environ.*, vol. 23, pp. 143–154, 1987.

[2] M. O. Smith, S. L. Ustin, J. B. Adams, and A. R. Gillespie, "Vegetation in deserts: II. Environmental influences on regional abundance," *Remote Sens. Environ.*, vol. 31, pp. 27–52, 1990.

[3] ——, "Vegetation in deserts: I. A regional measure of abundance from multispectral images," *Remote Sens. Environ.*, vol. 31, pp. 1–26, 1990.

[4] Y. Sohn and R. M. McCoy, "Mapping desert shrub rangeland using spectral unmixing and modeling spectral mixtures with TM data," *Photogramm. Eng. Remote Sens.*, vol. 63, pp. 707–716, 1997.

[5] A. J. Elmore, J. F. Mustard, S. J. Manning, and D. B. Lobell, "Quantifying vegetation change in semiarid environments: Precision and accuracy of spectral mixture analysis and the normalized difference vegetation index," *Remote Sens. Environ.*, vol. 73, pp. 87–102, 2000.

[6] F. J. Garcia-Haro, M. A. Gilabert, and J. Melia, "Linear spectral mixture modeling to estimate vegetation amount from optical spectral data," *Int. J. Remote Sens.*, vol. 17, pp. 3373–3400, 1996.

[7] S. G. Ungar, J. S Pearlman, J. Mendenhall, and D. Reuter, "Overview of the Earth Observing 1 (EO-1) mission," *IEEE Trans. Geosci. Remote Sensing*, vol. 41, June 2003.

[8] A. J. Elmore, J. F. Mustard, and S. J. Manning, "Regional patterns of plant community response to changes in water: Owens Valley, California," *Ecol. Appl.*, vol. 13, no. 2, pp. 436–460, 2003.

[9] F. L. Bookstein, "Principal warps: Thin-plate splines and the decomposition of deformations," *IEEE Trans. Pattern Anal. Machine Intell.*, vol. 11, pp. 567–585, June 1989.

[10] J. B. Adams, M. O. Smith, and P. E. Johnson, "Spectral mixture modeling: A new analysis of rock and soil types at the Viking Lander 1 site," *J. Geophys. Res.*, vol. 91, pp. 8098–8112, 1986.

[11] J. F. Mustard and C. M. Pieters, "Abundance and distribution of Ultramafic Microbreccia in Moses Rock Dike: Quantitative application of mapping spectrometer data," *J. Geophys. Res.*, vol. 92, pp. 13619–13 634, 1987.

[12] J. B. Adams, M. O. Smith, and A. R. Gillispie, "Imaging spectroscopy: Interpretations based on spectral mixture analysis," in *Remote Geochemical Analysis: Elemental and Mineralogical Composition*, C. M. Pieters and P. A. Englert, Eds. Cambridge, U.K.: Cambridge Univ. Press, 1993, pp. 145–166.

[13] J. F. Mustard and J. M. Sunshine, "Spectral analysis for earth science: Investigations using remote sensing data," in *Remote Sensing for the Earth Sciences: Manual of Remote Sensing*, 3rd ed, A. Rencz, Ed. New York: Wiley, 1999, vol. 3, ch. 5, pp. 251–307.

[14] J. R. Schott, C. Salvaggio, and W. J. Volchok, "Radiometric scene normalization using pseudoinvariant features," *Remote Sens. Environ.*, vol. 26, pp. 1–16, 1988.

[15] F. G. Hall, D. E. Strebel, J. E. Nickeson, and S. J. Goetz, "Radiometric rectification-toward a common radiometric response among multidate, multisensor images," *Remote Sens. Environ.*, vol. 35, pp. 11–27, 1991.

[16] H. F. Heady, R. P. Gibbens, and R. W. Powell, "A comparison of the charting, line intercept, and line-point methods of sampling shrub types of vegetation," *J. Range Manage.*, vol. 12, pp. 180–188, 1959.

[17] C. D. Bonham, *Measurements for Terrestrial Vegetation*. New York: Wiley, 1989, p. 338.

[18] S. K. Sorenson, P. D. Dileanis, and F. A. Branson, "Soil and vegetation responses to precipitation and changes in depth to groundwater in Owens Valley, California," U.S. Geological Survey, Water-Supply Paper 2370-G, 1991.

[19] K. J. Hollett, W. R. Danskin, W. F. McCaffrey, and C. L. Walti, "Geology and water resources of Owens Valley, California," U.S. Geological Survey, Water-Supply Paper 2370-B, 1991.

[20] C. G. Borel and S. A. W. Gerstl, "Nonlinear spectral mixing models for vegetative and soil surfaces," *Remote Sens. Environ.*, vol. 47, pp. 403–416, 1994.

[21] T. W. Ray and B. C. Murray, "Nonlinear spectral mixing in desert vegetation," *Remote Sens. Environ.*, vol. 55, pp. 59–64, 1996.

[22] A. R. Huete, R. D. Jackson, and D. F. Post, "Spectral response of a plant canopy with different soil backgrounds," *Remote Sens. Environ.*, vol. 17, pp. 37–53, 1985.

[23] R. P. Pech, R. D. Graetz, and A. W. Davis, "Reflectance modeling and the derivation of vegetation indices for an Australian semi-arid shrubland," *Int. J. Remote Sens.*, vol. 7, pp. 389–403, 1986.

[24] J. B. Adams, D. Sabol, V. Kapos, R. Almeida Filho, D. A. Roberts, M. O. Smith, and A. R. Gillespie, "Classification of multispectral images based on fractions of endmembers: Application to land-cover change in the Brazilian Amazon," *Remote Sens. Environ.*, vol. 52, pp. 137–154, 1995.

[25] D. A. Roberts, J. B. Adams, and M. O. Smith, "Discriminating green vegetation, nonphotosynthetic vegetation and soils in AVIRIS data," *Remote Sens. Environ.*, vol. 55, pp. 59–64, 1993.

[26] G. P. Asner and D. B. Lobell, "A biogeophysical approach for automated SWIR unmixing of soils and vegetation," *Remote Sens. Environ.*, vol. 74, pp. 99–112, 2000.

[27] J. A. Mendenhall *et al.*, "Earth Observing-1 Advanced Land Imager: Instrument and flight operations overview," Mass. Inst. Technol., Cambridge, MA, MIT/LL Project Rep. EO-1-1, June 23, 2000.

Andrew James Elmore received the Ph.D. degree from Brown University, Providence, RI, in 2003.

He is currently a Postdoctoral Research Associate with Department of Global Ecology, Carnegie Institution of Washington, Stanford, CA. His research interests include many aspects of global change research, including the land-use and land-cover applications of remote sensing data, the role of invasive species in global change, and informing sustainable water resource management.

John Fraser Mustard received the Ph.D. degree from Brown University, Providence, RI, in 1990.

He is currently an Associate Professor in the Department of Geological Sciences and Center for Environmental Studies, Brown University. His research ranges from surface composition and processes on Mars to environmental change on the earth. Recent research on the earth has focused on the drivers and impacts of environmental change in arid and semiarid regions, with an emphasis on water issues.